

Threshold-Based Fast Successive-Cancellation Decoding of Polar Codes

Haotian Zheng, *Student Member, IEEE*, Seyyed Ali Hashemi, *Member, IEEE*,
Alexios Balatsoukas-Stimming, *Member, IEEE*, Zizheng Cao, *Member, IEEE*, Ton Koonen, *Fellow, IEEE*,
John Cioffi, *Fellow, IEEE*, Andrea Goldsmith, *Fellow, IEEE*

Abstract—This paper focuses on developing fast successive-cancellation (SC) decoding methods for polar codes. Fast SC decoding overcomes the latency caused by the serial nature of the SC decoding by identifying new nodes in the upper levels of the SC decoding tree and implementing their fast parallel decoders. Our proposed methods consist of several new techniques. First, a novel sequence repetition node corresponding to a class of bit sequences is presented. Most existing special node types are special cases of the proposed sequence repetition node. Then a fast parallel decoder is proposed for this class of node. To further speed up the decoding process of general nodes outside this class, a threshold-based hard-decision-aided scheme is introduced. The threshold value that guarantees a given error-correction performance in the proposed scheme is derived theoretically. Analyses and simulations on a polar code of length 1024 and rate $1/2$ show that the fast decoding algorithm with the proposed node can provide 19% latency reduction at $E_b/N_0 = 2.0$ dB compared to the fastest SC decoding algorithm in literature without tangibly altering the error-correction performance of the code. In addition, with the help of the proposed threshold-based hard-decision-aided scheme, the decoding latency can be further reduced by 54% at $E_b/N_0 = 5.0$ dB.

Index Terms—Polar codes, Fast successive-cancellation decoding, Sequence repetition node, Threshold-based hard-decision-aided scheme.

I. INTRODUCTION

POLAR codes represent a channel coding scheme that can provably achieve the capacity of a binary-input memoryless channel [1]. The explicit coding structure and low-complexity successive-cancellation (SC) decoding algorithm has generated significant interest in polar code research across both industry and academia. In particular, in the latest cellular standard of 5G [2], polar codes are adopted in the control channel of the enhanced mobile broadband (eMBB) use case. Although SC decoding provides a low-complexity capacity-achieving solution for polar codes with long block length, its sequential bit-by-bit decoding nature leads to high decoding latency, which constrains its application in low-latency communication scenarios such as the ultra-reliable low-latency communication (URLLC) [2] scheme of 5G. Therefore, the

design of fast SC-based decoding algorithms for polar codes with low decoding latency has received a lot of attention [3].

A look-ahead technique was adopted to speed up the bit-by-bit SC decoding in [4], [5] by pre-computing all the possible likelihoods of the bits that have not been decoded yet, and selecting the appropriate likelihood once the corresponding bit is estimated. Using the binary tree representation of SC decoding of polar codes, instead of working at the bit-level which corresponds to the leaf nodes of the SC decoding tree, parallel multi-bit decision is performed at the intermediate nodes of the SC decoding tree. An exhaustive-search decoding algorithm is used in [6]–[9] to make multi-bit decisions and to avoid the latency caused by the traversal of the SC decoding tree to compute the intermediate likelihoods. However, due to the high complexity of the exhaustive search, this method is generally only suitable for nodes that represent codes of very short lengths.

It was shown in [10] that a node in the SC decoding tree that represents a code of rate 0 (Rate-0 node) or a code of rate 1 (Rate-1 node) can be decoded efficiently without traversing the SC decoding tree. In [11], fast decoders of repetition (REP) and single parity-check (SPC) nodes were proposed for the SC decoding. Techniques were developed in [12]–[15] to adjust the codes that are represented by the nodes in the SC decoding tree to increase the number of nodes that can be decoded efficiently. However, these methods result in a degraded error-correction performance. On the basis of the works in [10], [11], five new nodes (Type-I, Type-II, Type-III, Type-IV, and Type-V) were identified and their fast decoders were designed in [16]. In [17], a generalized REP (G-REP) node and a generalized parity-check (G-PC) node were proposed to reduce the latency of the SC decoding even further. In [18], seven of the most prevalent node patterns in short polar codes were analysed and efficient algorithms for processing these node patterns in parallel are proposed. However, the decoding of some of these node patterns leads to significant performance loss. All these works require the design of a separate decoder for each class of node, which inevitably increases the implementation complexity. In addition, as shown in this work, the achievable parallelism in decoding can be further increased without degrading the error-correction performance.

For general nodes that do not fall in one of the above node categories, [19] proposed a hard-decision scheme based on node error probability. Specifically, in that work it was shown that extra latency reduction can be achieved when the communications channel has low noise. However, the hard-

H. Zheng, A. Balatsoukas-Stimming, Z. Cao, and A. M. J. Koonen are with the Department of Electrical Engineering, Eindhoven University of Technology, The Netherlands (e-mails: {h.zheng, a.k.balatsoukas.stimming, z.cao, a.m.j.koonen}@tue.nl). (Corresponding author: Zizheng Cao)

S. A. Hashemi, J. Cioffi, and A. Goldsmith are with the Department of Electrical Engineering, Stanford University, Stanford, CA 94305 USA (e-mails: {ahashemi, cioffi}@stanford.edu, andrea@wsl.stanford.edu).

Part of this work is accepted for presentation at the IEEE International Conference on Communications, Dublin, Ireland, June 2020.

decision threshold is calculated empirically rather than for a desired error-correction performance. In [20], a hypothesis-testing-based strategy is designed to select reliable unstructured nodes for hard decision. However, additional operations are required to be performed to calculate the decision rule, thus, incurring extra decoding latency. For all the existing hard-decision schemes, a threshold comparison operation is required each time a general constituent code is encountered in the course of the SC decoding algorithm.

In this paper, a fast SC decoding algorithm with a higher degree of parallelism than the state of the art is proposed. First, a class of *sequence repetition* (SR) nodes is proposed which provides a unified description of most of the existing special nodes. This class of nodes is typically found at a higher level of the decoding tree than other existing special nodes. Utilizing this class of nodes, a fast simplified SC decoding algorithm called the *SR node-based fast SC* (SRFSC) decoding algorithm is proposed. The proposed SRFSC decoding algorithm achieves a higher degree of parallelism and has smaller latency than the state of the art, without degrading the error-correction performance. Performance results show that the proposed SRFSC decoder achieves up to 50%, 31%, and 29% latency reduction with respect to the decoders in [11], [16], and [17], respectively.

Second, a threshold-based hard-decision-aided (TA) scheme is proposed to speed up the decoding of the nodes that are not SR nodes for a binary additive white Gaussian noise (BAWGN) channel. Consequently, a TA-SRFSC decoding algorithm is proposed that adopts a simpler threshold for hard-decision than that in [19]. The effect of the defined threshold on the error-correction performance of the proposed TA-SRFSC decoding algorithm is analyzed. Moreover, a systematic way to derive the threshold value for a desired upper bound for its block error rate (BLER) is determined. Performance results show that, with the help of the proposed TA scheme, the decoding latency of SRFSC decoding can be further reduced by 54% at $E_b/N_0 = 5$ dB on a polar code of length 1024 and rate 1/2. To mitigate the possible error-correction performance loss caused by the proposed TA scheme, a multi-stage decoding strategy is introduced that achieves significant average latency reduction with negligible error-correction performance deterioration with respect to SRFSC decoding.

The rest of this paper is organized as follows. Section II gives a brief introduction to the basic concept of polar codes and fast SC decoding. In Section III, the SRFSC decoding algorithm is introduced. With the help of the proposed TA scheme, the TA-SRFSC decoding is presented in Section IV. Section V analyzes the decoding latency and simulation results are shown in Section VI. Finally, Section VII gives a summary of the paper and concluding remarks.

II. PRELIMINARIES

A. Notation Conventions

In this paper, blackboard letters, such as \mathbb{X} , denote a set and $|\mathbb{X}|$ denotes the number of elements in \mathbb{X} . Bold letters, such as \mathbf{v} , denote a row vector, \mathbf{v}^T denotes the transpose of

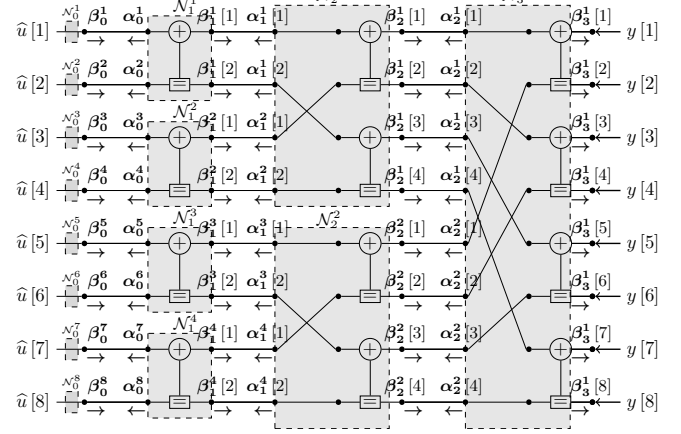


Fig. 1. SC decoding on the factor graph of a polar code with $N = 8$.

\mathbf{v} , and notation $\mathbf{v}[i:j]$, $1 \leq i < j$ represents a subvector $(v[i], v[i+1], \dots, v[j])$. \oplus is used as the bitwise XOR operation and $\mathbf{v}[i:j] \oplus \mathbf{z} = (v[i] \oplus z, v[i+1] \oplus z, \dots, v[j] \oplus z)$, $z \in \{0, 1\}$. The Kronecker product of two matrices \mathbf{F} and \mathbf{G} is written as $\mathbf{F} \otimes \mathbf{G}$. \mathbf{F}_N represents an $N \times N$ square matrix and $\mathbf{F}_N^{\otimes n}$ denotes the n -th Kronecker power of \mathbf{F}_N . Throughout this paper, $\ln(x)$ denotes the natural logarithm and $\log(x)$ indicates the base-2 logarithm of x , respectively.

B. Polar Codes

A polar code with code length $N = 2^n$ and information length K is denoted by $\mathcal{P}(N, K)$ and has rate $R = K/N$. The encoding process can be expressed as $\mathbf{x} = \mathbf{u}\mathbf{G}_N$, where $\mathbf{u} = (u[1], u[2], \dots, u[N])$ is the input bit sequence and $\mathbf{x} = (x[1], x[2], \dots, x[N])$ is the encoded bit sequence. $\mathbf{G}_N = \mathbf{R}_N \mathbf{F}_2^{\otimes n}$ is the generator matrix, where \mathbf{R}_N is a bit-reversal permutation matrix and $\mathbf{F}_2 = \begin{bmatrix} 1 & 0 \\ 1 & 1 \end{bmatrix}$.

The input bit sequence \mathbf{u} consists of K information bits and $N - K$ frozen bits. The information bits form set \mathbb{A} , transmitting information bits, while the frozen bits form set \mathbb{A}^c , transmitting fixed bits known to the receiver. For symmetric channels, without loss of generality, all frozen bits are set to zero [1]. To distinguish between frozen and information bits, a vector of flags $\mathbf{d} = (d[1], d[2], \dots, d[N])$ is used where each flag $d[k]$ is assigned as

$$d[k] = \begin{cases} 0, & \text{if } k \in \mathbb{A}^c, \\ 1, & \text{otherwise.} \end{cases} \quad (1)$$

The codeword \mathbf{x} is transmitted through a channel after modulation. In this paper, non-systematic polar codes and binary phase-shift keying (BPSK) modulation which maps $\{0, 1\}$ to $\{+1, -1\}$ are considered. Transmission takes place over an additive white Gaussian noise (AWGN) channel.

C. SC Decoding and Binary Tree Representation

SC decoding can be illustrated on the factor graph of polar codes as shown in Fig. 1. The factor graph consists of $n + 1$ levels and, by grouping all the operations that can be performed in parallel, SC decoding can be represented as the

traversal of a binary tree. This traversal is shown in Fig. 2, starting from the left side of the binary tree. At level j of the SC decoding tree with $n + 1$ levels, there are 2^{n-j} nodes ($0 \leq j \leq n$), and the i -th node at level j ($1 \leq i \leq 2^{n-j}$) of the SC decoding tree is denoted as \mathcal{N}_j^i . The left and the right child nodes of \mathcal{N}_j^i are \mathcal{N}_{j-1}^{2i-1} and \mathcal{N}_{j-1}^{2i} , respectively, as illustrated in Fig. 2. For \mathcal{N}_j^i , $\alpha_j^i[k]$, $1 \leq k \leq 2^j$, indicates the k -th input logarithmic likelihood ratio (LLR) value, and $\beta_j^i[k]$, $1 \leq k \leq 2^j$, denotes the k -th output binary hard-valued message. For the AWGN channel, the received vector $\mathbf{y} = (y[1], y[2], \dots, y[N])$ from the channel can be used to calculate the channel LLR as $2\mathbf{y}/\sigma^2$, where σ^2 is the variance of the Gaussian noise. SC decoding starts by setting $\alpha_n^1[1:N] = 2\mathbf{y}/\sigma^2$. A node will be activated once all its inputs are available. When LLR messages pass through a node in the factor graph which is indicated by the \oplus sign, the f function over the LLR domain is executed as

$$\alpha_{j-1}^{2i-1}[k] = f(\alpha_j^i[2k-1], \alpha_j^i[2k]), \quad (2)$$

and when LLR messages pass through a node in the factor graph which is indicated by the \boxplus sign, the g function over the LLR domain is executed as

$$\alpha_{j-1}^{2i}[k] = g(\alpha_j^i[2k-1], \alpha_j^i[2k], \beta_{j-1}^{2i-1}[k]), \quad (3)$$

where

$$f(x, y) = 2 \operatorname{arctanh}\left(\tanh\left(\frac{x}{2}\right) \tanh\left(\frac{y}{2}\right)\right), \quad (4)$$

$$g(x, y, u) = (-1)^u x + y. \quad (5)$$

The f function can be approximated as [21]

$$f(x, y) = \operatorname{sign}(x) \operatorname{sign}(y) \min(|x|, |y|). \quad (6)$$

When the LLR value of the k -th bit at level zero α_0^k , $1 \leq k \leq N$, is calculated, the estimation of $u[k]$, denoted as $\hat{u}[k]$, can be obtained as

$$\hat{u}[k] = \hat{\beta}_0^k = \begin{cases} 0, & \text{if } k \in \mathbb{A}^c, \\ \frac{1 - \operatorname{sign}(\alpha_0^k)}{2}, & \text{otherwise.} \end{cases} \quad (7)$$

The hard-valued messages are propagated back to the parent node as

$$\hat{\beta}_j^i[k] = \begin{cases} \hat{\beta}_{j-1}^{2i-1}[\frac{k+1}{2}] \oplus \hat{\beta}_{j-1}^{2i}[\frac{k+1}{2}], & \text{if } \operatorname{mod}(k, 2) = 1, \\ \hat{\beta}_{j-1}^{2i-1}[\frac{k}{2}], & \text{if } \operatorname{mod}(k, 2) = 0. \end{cases} \quad (8)$$

After traversing all the nodes in the SC decoding tree, $\hat{\mathbf{u}}$ contains the decoding result. Thus the latency of SC decoding for a polar code of length N in terms of the number of time steps can be represented by the number of nodes in the SC decoding tree as [1]

$$\mathcal{T}_{\text{SC}} = 2N - 2. \quad (9)$$

D. Fast SC Decoding

The SC decoding has strong data dependencies that limit the amount of parallelism that can be exploited within the algorithm because the estimation of each bit depends on the estimation of all previous bits. This leads to a large latency in

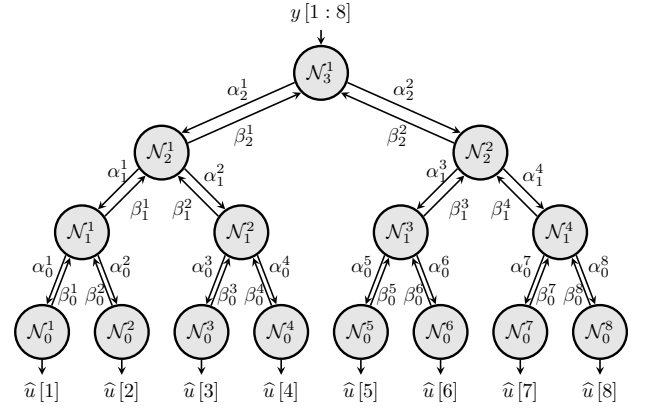


Fig. 2. Binary tree representation of a SC decoder for a polar code with $N = 8$.

the SC decoding algorithm. It was pointed out in [8] that for a node \mathcal{N}_j^i , $\beta_j^i[1:2^j]$ can be estimated without traversing the decoding tree by calculating

$$\hat{\beta}_j^i[1:2^j] = \arg \max_{\beta_j^i[1:2^j] \in \mathbb{C}_j^i} \sum_{k=1}^{2^j} (-1)^{\beta_j^i[k]} \alpha_j^i[k], \quad (10)$$

where \mathbb{C}_j^i is the set of all the codewords associated with node \mathcal{N}_j^i . Multibit decoding can be performed directly in an intermediate level instead of bit-by-bit sequential decoding at level 0, in order to traverse fewer nodes in the SC decoding tree and consequently, reducing the latency caused by data computation and exchange. However, the evaluation of (10) generally requires exhaustive search over all the codewords in the set \mathbb{C}_j^i which is computationally intensive in practice. In [11], a fast SC (FSC) decoding algorithm was proposed which performs fast parallel decoding when specific special node types are encountered. The sequences of information and frozen bits of these node types have special bit-patterns. Therefore, they can be decoded more efficiently without the need for exhaustive search. Using the vector \mathbf{d} , the four special node types proposed in [11] are described as:

- Rate-0 node: all bits are frozen bits, $\mathbf{d} = (0, 0, \dots, 0)$.
- Rate-1 node: all bits are non-frozen bits, $\mathbf{d} = (1, 1, \dots, 1)$.
- REP node: all bits are frozen bits except the last one, $\mathbf{d} = (0, \dots, 0, 1)$.
- SPC node: all bits are non-frozen bits except the first one, $\mathbf{d} = (0, 1, \dots, 1)$.

In [16], five additional special node types and their corresponding fast decoders were introduced. This enhanced FSC decoding algorithm can achieve a lower decoding latency than FSC decoding. The five special node types are:

- Type-I node: all bits are frozen bits except the last two, $\mathbf{d} = (0, \dots, 0, 1, 1)$.
- Type-II node: all bits are frozen bits except the last three, $\mathbf{d} = (0, \dots, 0, 1, 1, 1)$.
- Type-III node: all bits are non-frozen bits except the first two, $\mathbf{d} = (0, 0, 1, \dots, 1)$.
- Type-IV node: all bits are non-frozen bits except the first three, $\mathbf{d} = (0, 0, 0, 1, \dots, 1)$.

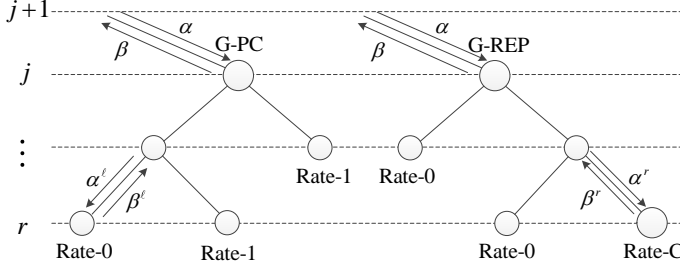


Fig. 3. General structures of G-PC node (left) and G-REP node (right).

- Type-V node: all bits are frozen bits except the last three and the fifth to last, $\mathbf{d} = (0, \dots, 0, 1, 0, 1, 1, 1)$.

A generalized FSC (GFSC) decoding algorithm was proposed in [17] by introducing the G-PC node and the G-REP node. The G-PC node is a node at level j having all its descendants as Rate-1 nodes except the leftmost one at a certain level $r < j$, that is a Rate-0 node. The G-REP node is a node at level j for which all its descendants are Rate-0 nodes, except the rightmost one at a certain level $r < j$, which is a generic node of rate C (Rate-C). The structures of G-PC and G-REP nodes are depicted in Fig. 3.

The key advantage of using specific parallel decoders for the aforementioned special nodes is that, since the SC decoding tree is not traversed when one of these nodes is encountered, significant latency saving can be achieved. For example, if \mathcal{N}_j^i is a Rate-1 node, hard decision decoding can be used to immediately obtain the decoding result as

$$\hat{\beta}_j^i[k] = h(\alpha_j^i[k]) = \begin{cases} 0, & \text{if } \alpha_j^i[k] \geq 0, \\ 1, & \text{otherwise.} \end{cases} \quad (11)$$

If \mathcal{N}_j^i is a SPC node, hard decision based on (11) is first derived followed by the calculation of the parity of the output using modulo-2 addition. The index of the least reliable bit is found as

$$k' = \arg \min_k |\alpha_j^i[k]|. \quad (12)$$

Finally, the bits in a SPC node are estimated as

$$\hat{\beta}_j^i[k] = \begin{cases} h(\alpha_j^i[k]) \oplus \text{parity}, & \text{if } k = k', \\ h(\alpha_j^i[k]), & \text{otherwise.} \end{cases} \quad (13)$$

This operation can be performed in a single time step [16]. Finally, if \mathcal{N}_j^i is a G-PC node, the decoding can be viewed as a parallel decoding of several separate SPC nodes. The decoding of a G-PC node can generally be performed in one time step considering parallel SPC decoders [17].

All of the aforementioned fast SC decoding algorithms perform parallel decoding at an intermediate level of the decoding tree in order to reduce the number of traversed nodes. In fact, a parallel decoding algorithm that can decode a node at a higher level of the decoding tree generally results in more savings in terms of latency than the one that decodes a node at a lower level of the decoding tree. This is due to the fact that a node at a higher level of the SC decoding tree has a

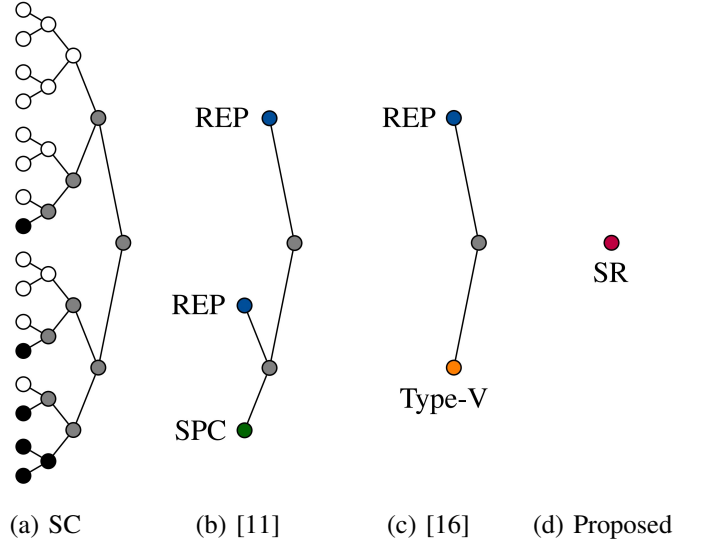


Fig. 4. Example of a decoding tree of the proposed SR node in comparison with different available special nodes.

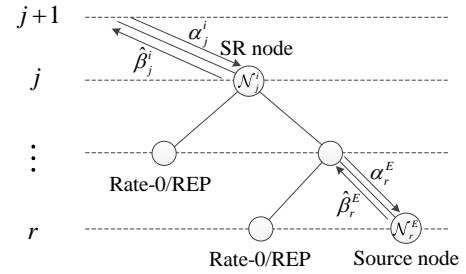


Fig. 5. General structure of a sequence repetition node.

longer length than the nodes below it. The following section introduces a class of nodes which is at a higher level of the SC decoding tree and shows how parallel decoding at this class of nodes can be exploited to achieve significant latency savings in comparison with the state of the art.

III. FAST SC DECODING WITH SEQUENCE REPETITION NODES

A. Sequence Repetition (SR) Node

Let \mathcal{N}_j^i be a node at level j of the binary tree representation of SC decoding as shown in Fig. 2. An SR node is any node at stage j for which all its descendants are either Rate-0 or REP nodes, except the rightmost one at a certain stage r , $0 \leq r \leq j$, that is a generic node of rate C . An example of a decoding tree of the proposed SR node in comparison with different available special nodes is illustrated in Fig. 4. The general structure of an SR node is depicted in Fig. 5. The rightmost node \mathcal{N}_r^E at stage r is denoted as the source node of the SR node \mathcal{N}_j^i . Let $E = i \times 2^{j-r}$ so the source node can be denoted as \mathcal{N}_r^E .

An SR node can be represented by three parameters as $\text{SR}(v, \text{SNT}, r)$, where r is the level of the SC decoding

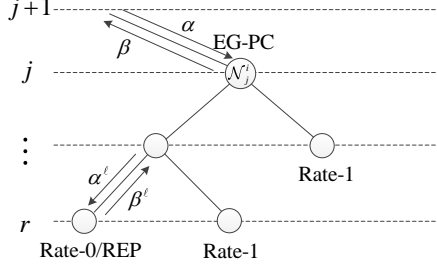


Fig. 6. General structure of Extended G-PC (EG-PC) Node.

tree in which \mathcal{N}_r^E is located, SNT is the source node type, and $\mathbf{v} = (v[j], v[j-1], \dots, v[r+1])$ is a vector of length $(j-r)$ such that for the left child node of the parent node of \mathcal{N}_r^E at level k , $r < k \leq j$, $v[k]$ is calculated as

$$v[k] = \begin{cases} 0, & \text{if the left child node is a Rate-0 node,} \\ 1, & \text{if the left child node is a REP node.} \end{cases} \quad (14)$$

Note that when $r = j$, \mathcal{N}_j^i is a source node and thus \mathbf{v} is an empty vector denoted as $\mathbf{v} = \emptyset$.

B. Source Node

To define the source node type, an extended class of G-PC (EG-PC) nodes is first introduced. The structure of the EG-PC node is depicted in Fig. 6. The EG-PC node is different from the G-PC node in its leftmost descendant node that can be either a Rate-0 or a REP node. The bits in an EG-PC node satisfy the following parity check constraint,

$$z = \bigoplus_{m=(k-1)2^{j-r}+1}^{k \times 2^{j-r}} \beta_j^i[m], \quad (15)$$

where $k \in \{1, \dots, 2^r\}$, and $z \in \{0, 1\}$ is the parity. Unlike G-PC nodes whose parity is always even ($z = 0$), the EG-PC node can have either even parity ($z = 0$) or odd parity ($z = 1$). The parity of the EG-PC node can be calculated as

$$z = \begin{cases} 0, & \text{if the leftmost node is Rate-0,} \\ h\left(\sum_{k=1}^{2^r} \alpha_k\right), & \text{otherwise,} \end{cases} \quad (16)$$

where $\alpha_k = 2 \tanh^{-1} \left(\prod_{m=(k-1)2^{j-r}+1}^{k \times 2^{j-r}} \tanh \left(\frac{\alpha_j^i[m]}{2} \right) \right)$. After computing z , Wagner decoders [22] can be used to decode the 2^r SPC codes with either even or odd parity constraints.

SPC, Type-III, Type-IV, and G-PC nodes can be represented as special cases of EG-PC nodes. As a result, most of the common special nodes can be represented as SR nodes where $\text{SNT} \in \{\text{Rate-0}, \text{Rate-1}, \text{EG-PC}, \text{Rate-C}\}$. Table I shows the corresponding representation of different node types at level j in the decoding tree as special cases of the SR nodes.

C. Repetition Sequence

In this subsection, a set of sequences, called repetition sequences, is defined that can be used to calculate the output

TABLE I
SR NODE REPRESENTATION OF COMMON NODE TYPES.

Node Type	SR Node Representation	Length of \mathbf{v}
Rate-0	$\text{SR}(\emptyset, \text{Rate-0}, j)$	0
REP	$\text{SR}((0, \dots, 0), \text{Rate-1}, 0)$	j
SPC	$\text{SR}(\emptyset, \text{EG-PC}, j)$	0
Rate-1	$\text{SR}(\emptyset, \text{Rate-1}, j)$	0
Type-I	$\text{SR}((0, \dots, 0), \text{Rate-1}, 1)$	$j-1$
Type-II	$\text{SR}((0, \dots, 0), \text{EG-PC}, 2)$	$j-2$
Type-III	$\text{SR}(\emptyset, \text{EG-PC}, j)$	0
Type-IV	$\text{SR}(\emptyset, \text{EG-PC}, j)$	0
Type-V	$\text{SR}((0, \dots, 0, 1), \text{EG-PC}, 2)$	$j-2$
G-PC	$\text{SR}(\emptyset, \text{EG-PC}, j)$	0
G-REP	$\text{SR}((0, \dots, 0), \text{Rate-C}, r)$	$j-r$

bit estimates of an SR node based on the output bit estimates of its source node. To derive the repetition sequences, \mathbf{v} is used to generate all the possible sequences that have to be XORed with the output of the source node to generate the output bit estimates of the SR node. Let η_k denote the rightmost bit value of the left child node of the parent node of \mathcal{N}_r^E at level $k+1$. When $v[k+1] = 0$, the left child node is a Rate-0 node so $\eta_k = 0$. When $v[k+1] = 1$, the left child node is a REP node, thus η_k can take the value of either 0 or 1. The number of repetition sequences is dependent on the number of different values that η_k can take. Let W_v denote the number of '1's in \mathbf{v} . The number of all possible repetition sequences is thus 2^{W_v} . Let $\mathbb{S} = \{s_1, \dots, s_{2^{W_v}}\}$ denote the set of all possible repetition sequences.

The output bits of SR node $\beta_j^i[1 : 2^j]$ have the property that their repetition sequence is repeated in blocks of length 2^{j-r} . Let $\beta_r^E[1 : 2^r]$ denote the output bits of the source node of an SR node \mathcal{N}_j^i . The output bits for each block of length 2^{j-r} in \mathcal{N}_j^i with respect to the output bits of its source node can be written as

$$\beta_j^i[(k-1)2^{j-r}+1 : k2^{j-r}] = \beta_r^E[k] \oplus s_l, \quad (17)$$

where $k \in \{1, \dots, 2^r\}$ and $s_l = \{s_l[1], \dots, s_l[2^{j-r}]\}$ is the l -th repetition sequence in \mathbb{S} . To obtain the repetition sequence s_l and with a slight abuse of terminology and notation for convenience, the Kronecker sum operator \boxplus is used, which is equivalent to the Kronecker product operator, except that addition in GF(2) is used instead of multiplication. For each set of values that η_k 's can take, s_l can be calculated as

$$s_l = (\eta_r, 0) \boxplus (\eta_{r+1}, 0) \boxplus \dots \boxplus (\eta_{j-1}, 0). \quad (18)$$

Example 1 (Repetition sequences for $\text{SR}((1, 1), \text{EG-PC}, 2)$). Consider the example in Fig. 4 in which the SR node \mathcal{N}_4^1 is located at level 4 of the decoding tree and its source node \mathcal{N}_2^4 is an EG-PC (in this case SPC) node located at level 2. Since $\mathbf{v} = (1, 1)$, $W_v = 2$ and $|\mathbb{S}| = 4$. For $\eta_1 \in \{0, 1\}$ and

$\eta_2 \in \{0, 1\}$,

$$\mathbf{s}_1 = (0, 0) \boxplus (0, 0) = (0, 0, 0, 0),$$

$$\mathbf{s}_2 = (1, 0) \boxplus (0, 0) = (1, 1, 0, 0),$$

$$\mathbf{s}_3 = (0, 0) \boxplus (1, 0) = (1, 0, 1, 0),$$

$$\mathbf{s}_4 = (1, 0) \boxplus (1, 0) = (0, 1, 1, 0).$$

■

For a polar code with a given \mathbf{d} , the locations of SR nodes in the decoding tree are fixed and can be determined off-line. Therefore, the repetition sequences in \mathbb{S} of all of the SR nodes can be pre-computed and used in the course of decoding.

D. Decoding of SR Nodes

To decode SR nodes, the LLR values $\alpha_{r_l}^E[1 : 2^r]$ of the source node \mathcal{N}_r^E are calculated based on the LLR values $\alpha_j^i[1 : 2^j]$ of the SR node \mathcal{N}_j^i for every repetition sequence \mathbf{s}_l by the following proposition:

Proposition 1. Let $\alpha_j^i[1 : 2^j]$ be the LLR values of the SR node \mathcal{N}_j^i and $\alpha_{r_l}^E[1 : 2^r]$ be the LLR values of its source node \mathcal{N}_r^E associated with the l -th repetition sequence \mathbf{s}_l . For $k \in \{1, \dots, 2^r\}$ and $l \in \{1, \dots, 2^{W_v}\}$,

$$\alpha_{r_l}^E[k] = \sum_{m=1}^{2^{j-r}} \alpha_j^i[(k-1)2^{j-r} + m] (-1)^{s_l[m]}. \quad (19)$$

Proof: See Appendix A. ■

Using (17) and (19), (10) can be written as

$$\begin{aligned} \hat{\beta}_j^i[1 : 2^j] &= \arg \max_{\beta_j^i[1:2^j] \in \mathbb{C}_j^i} \sum_{k=1}^{2^j} (-1)^{\beta_j^i[k]} \alpha_j^i[k] \\ &= \arg \max_{\substack{\beta_r^E[1:2^r] \in \mathbb{C}_r^E \\ \mathbf{s}_l \in \mathbb{S}}} \sum_{k=1}^{2^r} (-1)^{\beta_r^E[k]} \sum_{m=1}^{2^{j-r}} \alpha_{ji}^i[(k-1)2^{j-r} + m] (-1)^{s_l[m]} \\ &= \arg \max_{\substack{\beta_r^E[1:2^r] \in \mathbb{C}_r^E \\ l \in \{1, \dots, |\mathbb{S}|\}}} \sum_{k=1}^{2^r} (-1)^{\beta_r^E[k]} \alpha_{r_l}^E[k]. \end{aligned} \quad (20)$$

Thus, the bit estimates of an SR node $\hat{\beta}_j^i[1 : 2^j]$ can be calculated by finding the bit estimates of its source node $\beta_r^E[1 : 2^r]$ using (20) and the repetition sequences as shown in (17).

The decoding algorithm of an SR node \mathcal{N}_j^i is described in Algorithm 1. It first computes $\alpha_{r_l}^E$ for $l \in \{1, \dots, |\mathbb{S}|\}$ and generates $|\mathbb{S}|$ new paths by extending the decoding path at the $j-r$ rightmost bits corresponding to $\eta_r, \eta_{r+1}, \dots, \eta_{j-1}$. Note that the l -th path is generated when the repetition sequence is \mathbf{s}_l and $\alpha_{r_l}^E$, $\hat{\beta}_{r_l}^E$, and $\hat{\beta}_{ji}^i$ are its soft and hard messages. Then, the source node is decoded under the rule of the SC decoding. If the source node is a special node, a hard decision is made directly. Parity check and bit flipping will be performed further using Wagner decoder if the source node is an EG-PC node. Finally, the optimal decoding path index can be selected according to the comparison in (21) and the decoding result is obtained according to (17).

Based on Algorithm 1, the SR node-based fast SC (SRFSC) decoding algorithm is proposed. It follows the SC decoding algorithm schedule until an SR node is encountered where Algorithm 1 is executed. Note that the path selection operation in step 3 can be performed in parallel with the decoding of the source node in step 2 and the following g function. Once the selected index \hat{l} is obtained, only the l -th decoding path will be retained and the remaining paths will be deleted.

Algorithm 1: Decoding algorithm of SR node \mathcal{N}_j^i

Input: $\alpha_j^i[1 : 2^j], \mathbb{S};$

Output: $\hat{\beta}_j^i[1 : 2^j];$

1) Soft message computation

for $l \in \{1, \dots, |\mathbb{S}|\}$ **do**

 Calculate $\alpha_{r_l}^E$ according to (19).

end

2) Decoding of source node \mathcal{N}_r^E

for $l \in \{1, \dots, |\mathbb{S}|\}$ **do**

if $SNT=Rate-C$ **then**

 Decode source node \mathcal{N}_r^E using $\alpha_{r_l}^E$ and obtain $\hat{\beta}_{r_l}^E$.

else

if $SNT=Rate-0$ **then**

$\hat{\beta}_{r_l}^E[k] = 0, k \in \{1, \dots, 2^r\}$,

else

$\hat{\beta}_{r_l}^E[k] = h(\alpha_{r_l}^E[k]), k \in \{1, \dots, 2^r\}$.

end

end

if $SNT=EG-PC$ **then**

 Perform parity check and bit flipping on $\hat{\beta}_{r_l}^E$ using $\alpha_{r_l}^E$.

end

end

3) Comparison and path selection

$$\hat{l} = \arg \max_{l \in \{1, \dots, |\mathbb{S}|\}} \sum_{k=1}^{2^r} |\alpha_{r_l}^E[k]|. \quad (21)$$

Return $\hat{\beta}_{ji}^i$ to parent node according to (17).

IV. HARD-DECISION-AIDED FAST SC DECODING WITH SEQUENCE REPETITION NODES

In this section, a novel threshold-based hard-decision-aided scheme is proposed for the BAWGN channel. The purpose of this algorithm is to speed up the decoding of general nodes with no specific structure in the SRFSC decoding, especially when the transmission channel has low noise. Additionally, a multi-stage decoding strategy is introduced to eliminate the possible error-correction performance degradation caused by the proposed TA scheme.

A. Threshold-based Hard-decision-aided Scheme

For a BAWGN channel with standard deviation σ_n , it was shown in [23] that, considering all the previous bits are

decoded correctly, the LLR value $\alpha_j^i[k]$, $1 \leq k \leq 2^j$, input into node \mathcal{N}_j^i can be approximated as a Gaussian variable using a Gaussian approximation as

$$\alpha_j^i[k] \sim \mathcal{N}(M_j^i[k], 2|M_j^i[k]|), \quad (22)$$

where $M_j^i[k]$ is the expectation of $\alpha_j^i[k]$ [24] such that

$$M_j^i[k] = \begin{cases} m_j^i, & \text{if } \beta_j^i[k] = 0, \\ -m_j^i, & \text{if } \beta_j^i[k] = 1, \end{cases} \quad (23)$$

and m_j^i can be calculated recursively offline assuming the all-zero codeword is transmitted as

$$m_n^1 = 2/\sigma_n^2, \quad (24)$$

$$m_{j-1}^{2^i-1} = \varphi^{-1}(1 - [1 - \varphi(m_j^i)]^2), \quad (25)$$

$$m_{j-1}^{2^i} = 2m_j^i, \quad (26)$$

where

$$\varphi(x) = \begin{cases} 1 - \frac{1}{\sqrt{4|x|}} \int_{-\infty}^{\infty} \tanh\left(\frac{u}{2}\right) e^{-\frac{(u-x)^2}{4|x|}} du, & x \neq 0, \\ 0, & x = 0. \end{cases} \quad (27)$$

It was shown in [19] that, when the magnitude of the LLR values at a certain node in the SC decoding tree is large enough, the node has enough reliability to perform hard decision directly at the node without tangibly altering the error-correction performance. To determine the reliability of the node, a threshold is defined in [19] as

$$T = c_t \log \frac{1 - \frac{1}{2} \operatorname{erfc}\left(0.5\sqrt{m_j^i}\right)}{\frac{1}{2} \operatorname{erfc}\left(0.5\sqrt{m_j^i}\right)}, \quad (28)$$

where $c_t \geq 1$ is a constant that is selected empirically. The hard-decision estimate of the received LLR values is calculated using

$$\text{HB}_j^i[k] = \begin{cases} 0, & \text{if } \alpha_j^i[k] > T, \\ 1, & \text{if } \alpha_j^i[k] < -T. \end{cases} \quad (29)$$

Fig. 7 shows the distribution of $\alpha_j^i[k]$ under the Gaussian approximation. The red area represents the probability of correct hard decision P_c and the blue area represents the probability of incorrect hard decision P_e when $\beta_j^i[k] = 0$ such that

$$P_c = Q\left(\frac{T - m_j^i}{\sqrt{2m_j^i}}\right), \quad (30)$$

$$P_e = Q\left(\frac{T + m_j^i}{\sqrt{2m_j^i}}\right), \quad (31)$$

where

$$Q(x) = \frac{1}{\sqrt{2\pi}} \int_x^{\infty} e^{-\frac{t^2}{2}} dt. \quad (32)$$

The area between the two dashed lines represents the probability that a hard decision is not performed, which is equal to $1 - P_c - P_e$.

The issue with the method in [19] is that the threshold defined in (28) contains complex calculations of complementary

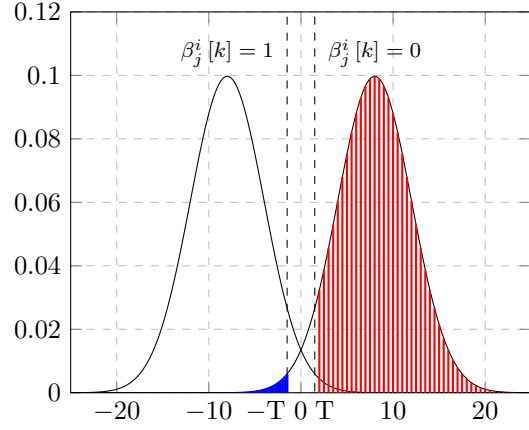


Fig. 7. Probability distribution of $\alpha_j^i[k]$ under Gaussian approximation for $m_j^i = 8$. The red dashed area on the right represents the probability of correct hard decision and the blue solid area on the left represents the probability of incorrect hard decision when $\beta_j^i[k] = 0$.

error functions $\operatorname{erfc}(\cdot)$, making the calculation in (30) and (31) inefficient. Moreover, the hard-decision threshold is calculated empirically rather than for a desired error-correction performance and the threshold comparison in (29) is performed every time an unstructured node is encountered in the SC decoding process. To simplify the calculation of the threshold and also solve the other two problems, we take a different approach than [19] by using the Gaussian distribution of $\alpha_j^i[k]$ in Fig. 7 and constrain the probability of error when $\beta_j^i[k] = 0$ to be

$$P_e = Q\left(\frac{T + m_j^i}{\sqrt{2m_j^i}}\right) < Q(c), \quad (33)$$

where c (and thus $Q(c)$) is a positive constant, whose selection method will be given in Proposition 2. This is equivalent to

$$T > -m_j^i + c\sqrt{2m_j^i}. \quad (34)$$

Therefore, the threshold can be written as

$$T = \left| -m_j^i + c\sqrt{2m_j^i} \right|, \quad (35)$$

where the absolute value ensures T is positive for all values of $m_j^i > 0$ with any $c > 0$.

For a node that undergoes hard decision in (29), the proposed threshold leads to a bounded probability of hard decision error as shown in the following proposition.

Proposition 2. Let $0 < \varepsilon < 1$ and $c > 0$ be real numbers such that

$$Q(c) \leq 1 - 2^n \varepsilon. \quad (36)$$

Performing hard decision in (29) with the threshold in (35) on nodes \mathcal{N}_j^i whose m_j^i satisfy

$$m_j^i \geq \frac{1}{2} \left[c - Q^{-1}\left(\frac{Q(c)}{2^n \varepsilon} - 1\right) \right]^2, \quad (37)$$

results in a probability of hard-decision error that is upper bounded by $1 - \varepsilon$ for any ε close to 1.

Proof: See Appendix B. ■

The proposed TA scheme performs hard decision on a node \mathcal{N}_j^i only if (37) is satisfied. Since (37) is calculated offline, only a fraction of nodes undergo hard decision in the decoding process, which avoids unnecessary threshold comparisons. Furthermore, a hard decision is performed on a node if all of its input LLR values $\alpha_j^i[k]$ satisfy (29). Otherwise, standard SC decoding is applied on \mathcal{N}_j^i to obtain the decoding result. To speed up the decoding process, the proposed TA scheme is combined with SRFSC decoding that results in the *threshold-based hard-decision-aided SR node-based fast SC* (TA-SRFSC) decoding algorithm. In TA-SRFSC decoding, when one of the special nodes considered in SRFSC decoding is encountered, SRFSC decoding is performed and when a general node with no special structure is encountered, the proposed TA scheme is applied. The following proposition provides an upper bound on the BLER of the proposed TA-SRFSC decoding.

Proposition 3. Let $\text{BLER}_{\text{TA-SRFSC}}$ and $\text{BLER}_{\text{SRFSC}}$ denote the BLER of the TA-SRFSC decoding and the SRFSC decoding respectively. The following holds

$$\text{BLER}_{\text{TA-SRFSC}} \leq 1 - \varepsilon(1 - \text{BLER}_{\text{SRFSC}}). \quad (38)$$

Proof: See Appendix C. ■

Proposition 3 provides a method to derive the threshold value for a desired upper bound of the BLER for TA-SRFSC decoding. In fact, a large threshold value results in a better error-correction performance than a small threshold value. However, since a large threshold value allows for only a few nodes to undergo hard decision in (29), this error-correction performance gain is obtained at the cost of lower decoding speed. Therefore, a trade-off between the error-correction performance and the decoding speed can be achieved with the proposed TA-SRFSC decoding algorithm.

B. Multi-stage Decoding

To mitigate the effect of the proposed TA scheme on the error-correction performance of the TA-SRFSC decoding, a multi-stage decoding strategy is adopted in which a maximum of two decoding attempts is conducted. In the first decoding attempt, TA-SRFSC decoding is adopted. If this decoding fails and if there existed a node that underwent hard decision in this first decoding attempt, then a second decoding attempt using the SRFSC decoding is conducted. To determine if the TA-SRFSC decoding failed, a cyclic redundancy check (CRC) is concatenated to the polar code and it is verified after the TA-SRFSC decoding. Additionally, the CRC is verified after the second decoding attempt by the SRFSC decoding to determine if the overall decoding process succeeded.

As shown in the next section, most of the received frames are decoded correctly by the proposed TA-SRFSC decoding in the first decoding attempt. As a result, the average decoding latency of the proposed multi-stage SRFSC decoding is very close to that of the TA-SRFSC decoding, while its error-correction performance is very close to that of SRFSC decoding. It is worth noting that the proposed multi-stage decoding strategy can be generalized to have more than two decoding

attempts. In this scenario the first two attempts are the same as described above, TA-SRFSC decoding is used first followed by SRFSC decoding on nodes that underwent hard decision. The third and any subsequent attempts would use increasingly more powerful decoding techniques than the first two, such as successive-cancellation list (SCL) decoding.

V. DECODING LATENCY

In this section, the decoding latency of the proposed fast decoders measured in terms of the number of time steps is analyzed using the same assumptions as in [1], [16]. More specifically:

- 1) There is no resource limitation so that all the parallelizable instructions are performed in one time step.
- 2) Bit operations are carried out instantaneously.
- 3) Addition/subtraction of real numbers and check-node operation consume one time step.
- 4) Wagner decoding can be performed in one time step.

A. SRFSC and TA-SRFSC

For any node \mathcal{N}_j^i that is not an SR node and that satisfies (37), the threshold comparison in (29) is performed in parallel with the calculation of the LLR values of its left child node. Therefore, the proposed hard decision scheme does not introduce overhead in the latency requirements for the nodes that undergo hard decision.

The number of time steps required for the decoding of the SR node is calculated according to Algorithm 1. In Step 1, the calculation of the LLR values for the source node requires one time step if $\mathbf{v} \neq \emptyset$. If $\mathbf{v} = \emptyset$, then the LLR values of the source node are available immediately. Thus, the required number of time steps for Step 1 is

$$\mathcal{T}_1 = \begin{cases} 0, & \text{if } \mathbf{v} = \emptyset, \\ 1, & \text{if } \mathbf{v} \neq \emptyset. \end{cases} \quad (39)$$

The time step requirement of Step 2 depends on the source node type. If SNT = Rate-C, the time step requirement of Step 2 is the time step requirement of the Rate-C node. If SNT = Rate-0 or Rate-1, then there is no latency overhead in Step 2. If SNT = EG-PC and in accordance with Section III-B, z can be estimated in two time steps if the leftmost node is a REP node (one time step for performing the check-node operation and one time step for adding the LLR values). Also, Wagner decoding can be performed in parallel with the estimation of z assuming $z = 0$ or $z = 1$. As such, at most two time steps are required for parity check and bit flipping of the EG-PC node. The required number of time steps for Step 2 is

$$\mathcal{T}_2 = \begin{cases} 0, & \text{if SNT = Rate-0 or Rate-1,} \\ 1 \text{ or } 2, & \text{if SNT = EG-PC,} \\ 2^{r+1} - 2, & \text{if SNT = Rate-C.} \end{cases} \quad (40)$$

Step 3 consumes two time steps using an adder tree and a comparison tree if $|\mathcal{S}| > 1$. If $|\mathcal{S}| = 1$, then there is no latency overhead in Step 3. Thus, the required number of time steps for Step 3 is

$$\mathcal{T}_3 = \begin{cases} 0, & \text{if } |\mathcal{S}| = 1, \\ 2, & \text{if } |\mathcal{S}| > 1. \end{cases} \quad (41)$$

Since path selection in Step 3 can be executed in parallel with the decoding of source node in Step 2 and the following g function calculation, the total number of time steps required to decode an SR node can be expressed as

$$\mathcal{T}_{\text{SR}} = \mathcal{T}_1 + \max(\mathcal{T}_2, \mathcal{T}_3 - 1), \quad (42)$$

where $\mathcal{T}_3 - 1$ indicates that at least one time step in \mathcal{T}_3 can be reduced by parallelizing Step 3 and the g function calculation. Therefore, \mathcal{T}_{SR} is a variable that is dependent on its parameters. However, with a given polar code, the total number of time steps required for the decoding of the polar code using SRFSC decoding is fixed, regardless of the channel conditions.

B. Multi-stage SRFSC

Let $\mathcal{T}_{\text{TA-SRFSC}}$ and $\mathcal{T}_{\text{SRFSC}}$ denote the average decoding latency of the proposed TA-SRFSC decoding and the SRFSC decoding, respectively, in terms of the number of required time steps. The average decoding latency of the proposed multi-stage SRFSC decoding, $\mathcal{T}_{\text{Multi-stage SRFSC}}$, is given by

$$\mathcal{T}_{\text{Multi-stage SRFSC}} = \mathcal{T}_{\text{TA-SRFSC}} + P_{\text{Re-decoding}} \mathcal{T}_{\text{SRFSC}}, \quad (43)$$

where $P_{\text{Re-decoding}}$ indicates the probability that TA-SRFSC decoding fails and there is at least one node that undergoes hard decision in the TA-SRFSC decoding. Note that $P_{\text{Re-decoding}}$ is less than or equal to the probability that the output of TA-SRFSC decoding fails the CRC verification, which can be approximated by $\text{BLER}_{\text{TA-SRFSC}}$. The approximation is due to the fact that the undetected error probability of CRC is negligible [25]. In accordance with Proposition 3, the approximate average decoding latency requirement for the proposed multi-stage SRFSC decoding can be derived as

$$\begin{aligned} \mathcal{T}_{\text{Multi-stage SRFSC}} \\ \lesssim \mathcal{T}_{\text{TA-SRFSC}} + (1 - \varepsilon(1 - \text{BLER}_{\text{SRFSC}})) \mathcal{T}_{\text{SRFSC}}. \end{aligned} \quad (44)$$

Note that the decoding latency of SRFSC decoding is fixed. Therefore, the average decoding latency and the worst case decoding latency of SRFSC decoding are equivalent. The worst case decoding latency of the proposed TA-SRFSC decoding can be calculated when none of the nodes in the decoding tree undergo hard decision. This occurs when the channel has a high level of noise. Thus, the worst case decoding latency of the proposed TA-SRFSC decoding is equivalent to the decoding latency of the SRFSC decoding. Moreover, when the channel is too noisy, $P_{\text{Re-decoding}} \approx 0$, because almost none of the nodes undergo hard decision. Thus, the worst case decoding latency of the proposed multi-stage SRFSC decoding is equivalent to the worst case decoding latency of TA-SRFSC decoding, which is the latency of SRFSC decoding.

VI. NUMERICAL RESULTS

In this section, the average decoding latency and the error-correction performance of the proposed decoding algorithms are analyzed and compared with state-of-the-art fast SC decoding algorithms. To derive the results, polar codes of length $N \in \{128, 512, 1024\}$, which are adopted in the 5G standard

TABLE II
THE NUMBER OF SR NODES WITH DIFFERENT $|\mathcal{S}|$ IN 5G POLAR CODES OF LENGTHS $N \in \{128, 512, 1024\}$ AND RATES $R \in \{1/4, 1/2, 3/4\}$.

N	R	$ \mathcal{S} $					Total
		1	2	4	8	16	
128	1/4	5	1	0	1	0	7
	1/2	5	1	1	1	0	8
	3/4	3	0	1	0	0	4
512	1/4	11	3	3	1	0	18
	1/2	17	3	3	1	0	24
	3/4	15	3	2	0	0	20
1024	1/4	17	4	3	2	1	27
	1/2	24	8	4	1	1	38
	3/4	26	7	2	1	0	36

[26], are used and a total of 10^7 frames are tested. The CRC of length 16, which is adopted in the 5G standard with generator polynomial $D^{16} + D^{12} + D^5 + 1$, is used for all transmitted frames to identify whether the decoding succeeded or failed. For the sake of fairness, the latency of other baseline decoding algorithms in the simulations are also calculated under the same assumptions in Section V.

To simulate the effect of ε on the error-correction performance and the latency of the proposed decoding algorithms, three values of $\varepsilon \in \{0.9, 0.99, 0.999\}$ are selected. In accordance with (36), $c \geq 3.8$ for $\varepsilon = 0.9$, $c \geq 4.3$ for $\varepsilon = 0.99$, and $c \geq 4.8$ for $\varepsilon = 0.999$. According to (33), with the increasing of c , P_e decreases which means less nodes will be performed hard decision and the decoding latency will increase. To get a tradeoff between error-correction performance and latency reduction, we set $c = 3.8$ for $\varepsilon = 0.9$, $c = 4.3$ for $\varepsilon = 0.99$, and $c = 4.8$ for $\varepsilon = 0.999$. Consequently, $m_j^i \geq 9.3891$ for $\varepsilon = 0.9$, $m_j^i \geq 14.7255$ for $\varepsilon = 0.99$, and $m_j^i \geq 16.1604$ for $\varepsilon = 0.999$ in accordance with (37). Using these values, the threshold T defined in (35), the BLER upper bound for the TA-SRFSC decoding in (38), and the approximate average decoding latency upper bound for the multi-stage SRFSC decoding in (44) can be calculated for different values of ε .

Table II reports the number of SR nodes with different $|\mathcal{S}|$ at different code lengths and rates. It can be seen that when the code length is 128, 512, and 1024, the codes with rate 1/2, 1/4, and 1/4 have the largest proportion of nodes with $|\mathcal{S}| > 1$, respectively. This in turn results in more latency savings because a higher degree of parallelism can be exploited with these nodes. Table III shows the length of SR nodes with different $|\mathcal{S}|$ at different code lengths when $R = 1/2$. The length of the SR nodes in the decoding tree corresponds to the level in the decoding tree that they are located. SR nodes with larger $|\mathcal{S}|$ that are located on a higher level of the decoding tree contribute more in the overall latency reduction.

Table IV reports the number of time steps required to decode polar codes of lengths $N \in \{128, 512, 1024\}$ and rates $R \in \{1/4, 1/2, 3/4\}$ with the proposed SRFSC decoding algorithm, and compares it with the required number of time

TABLE III
NODE LENGTH OF SR NODES WITH DIFFERENT $|\mathcal{S}|$ IN 5G POLAR CODES
OF LENGTHS $N \in \{128, 512, 1024\}$ AND RATE $R = 1/2$.

N	Node Length	$ \mathcal{S} $				
		1	2	4	8	16
128	4	1	1	0	0	0
	8	1	0	0	0	0
	16	2	0	1	0	0
	32	1	0	0	1	0
512	8	5	3	0	0	0
	16	5	0	3	0	0
	32	5	0	0	1	0
	64	2	0	0	0	0
1024	8	10	6	0	0	0
	16	6	1	3	0	0
	32	3	0	1	1	0
	64	3	1	0	0	1
	128	2	0	0	0	0

TABLE IV
NUMBER OF TIME STEPS FOR DIFFERENT FAST SC DECODING
ALGORITHMS OF POLAR CODES OF LENGTHS $N \in \{128, 512, 1024\}$ AND
RATES $R \in \{1/4, 1/2, 3/4\}$.

N	R	[11]	[16]	[17]	SRFSC
128	1/4	40	29	29	21
	1/2	46	35	34	24
	3/4	20	15	14	11
512	1/4	112	75	75	58
	1/2	126	92	89	75
	3/4	104	70	68	63
1024	1/4	178	127	121	89
	1/2	222	154	154	124
	3/4	186	128	126	111

steps of the decoders in [11], [16], and [17]. The proposed SRFSC decoder provides up to 50% latency reduction with respect to the decoder in [11], up to 31% latency reduction with respect to the decoder in [16], and up to 29% latency reduction with respect to the decoder in [17].

Table V compares the number of special nodes of polar codes with $N = 1024$ and $R = \{1/4, 1/2, 3/4\}$ for the proposed SRFSC decoding algorithm and the decoders in [11], [16], and [17]. It can be seen that the proposed SRFSC decoding algorithm has the minimum number of special node types and total number of nodes, since SR nodes are located at a higher level of the decoding tree.

Fig. 8 and Fig. 9, respectively, show the BLER and BER performance of different decoding algorithms when $N = 1024$ and $R = 1/2$, for different values of energy per bit to noise power spectral density ratio (E_b/N_0). For each value of ε , the BLER of TA-SRFSC decoding is depicted together with the upper bound calculated by Proposition 3. It can be seen that the introduction of the TA scheme results in BLER performance loss for the proposed TA-SRFSC decoding with respect to SC

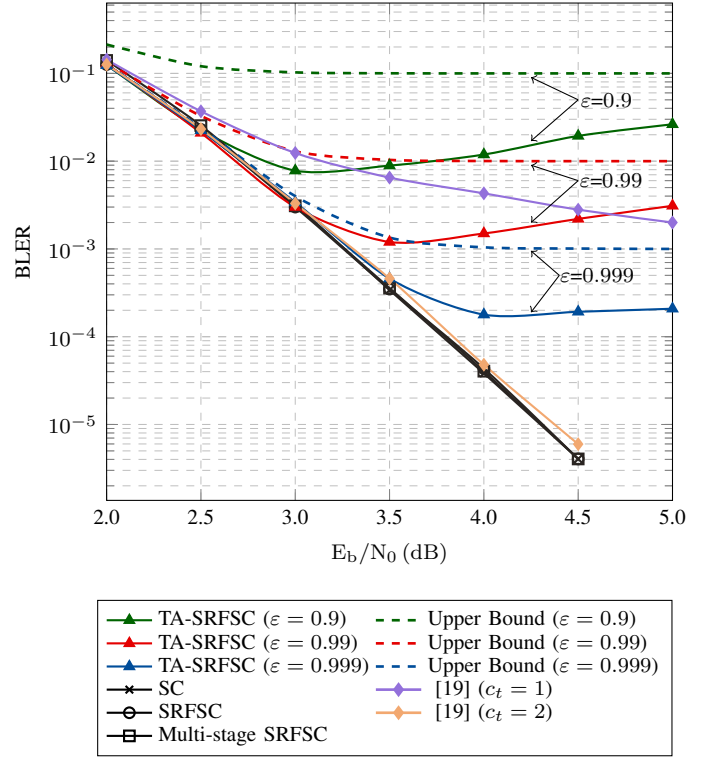


Fig. 8. BLER performance of different decoding algorithms for the 5G polar code of length $N = 1024$ and rate $R = 1/2$.

and SRFSC decoding, especially at higher values of E_b/N_0 . Moreover, the simulations confirm that the BLER curves of TA-SRFSC decoding fall below their respective upper bounds. It can also be seen that, as the E_b/N_0 value increases beyond a specific point, the BLER/BER performance of the TA-SRFSC decoding degrades. This is because of the difference in the performance of hard-decision and soft-decision decoding. In accordance with (37), more nodes undergo hard decision decoding for larger values of E_b/N_0 . Therefore, while the channel conditions improve, the hard decision decoding introduces errors that reduce the error-correction performance gain associated with these large E_b/N_0 values. As a result, the BLER/BER performance degrades after a certain value of E_b/N_0 . This phenomenon exists as long as there are nodes that can undergo hard decision decoding. After all the nodes are decoded using hard decision, the BLER/BER performance improves again as E_b/N_0 increases.

For all values of ε , the proposed multi-stage SRFSC decoding results in almost the same BLER/BER performance. Therefore, only one curve is plotted in Fig. 8 and Fig. 9 for the multi-stage SRFSC decoding. It shows negligible performance deterioration compared to the conventional SC and SRFSC decoders and provides a better BLER/BER performance than the method in [19] for $c_t \in \{1, 2\}$. A similar trend can also be observed when comparing the BLER/BER performance of different schemes for polar codes of other lengths and rates.

Fig. 10 presents the average decoding latency in terms of the required number of time steps for the proposed TA-SRFSC decoding, with and without multi-stage decoding.

TABLE V
NUMBER OF SPECIAL NODES FOR DIFFERENT DECODING ALGORITHMS OF POLAR CODES OF LENGTH $N = 1024$ AND WITH RATE $R = \{1/4, 1/2, 3/4\}$.

	R	Rate-0	Rate-1	SPC	REP	Type-I	Type-II	Type-III	Type-IV	Type-V	G-PC	G-REP	SR
[11]	1/4	18	15	16	22								
	1/2	17	17	26	26	—	—	—	—	—	—	—	—
	3/4	11	26	21	17								
[16]	1/4	3	2	7	13	2	2	3	2	7			
	1/2	0	4	12	12	2	2	2	2	12	—	—	—
	3/4	1	7	11	7	1	2	3	2	8			
[17]	1/4		2								19	19	
	1/2	—	4	—	—	—	—	—	—	—	26	18	—
	3/4		7								23	12	
SRFSC	1/4												27
	1/2	—	—	—	—	—	—	—	—	—	—	—	38
	3/4												36

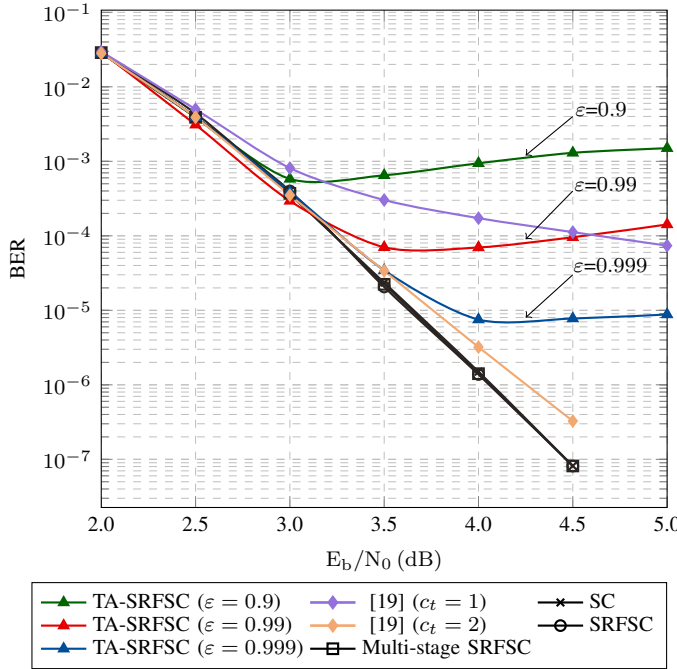


Fig. 9. BER performance of different decoding algorithms for the 5G polar code of length $N = 1024$ and rate $R = 1/2$.

In particular, it compares them with the latency of SRFSC decoding and the decoder in [19] at different values of E_b/N_0 when $N = 1024$ and $R = 1/2$. It can be seen that the required number of time steps for the proposed TA-SRFSC decoding decreases as E_b/N_0 increases and is reduced by 36% for $\varepsilon = 0.999$, by 45% for $\varepsilon = 0.99$, and by 54% for $\varepsilon = 0.9$, compared to SRFSC decoding at $E_b/N_0 = 5$ dB. The required number of time steps for the proposed multi-stage SRFSC decoding is close to that of the TA-SRFSC decoding and outperforms the method in [19] with $c_t = 1$

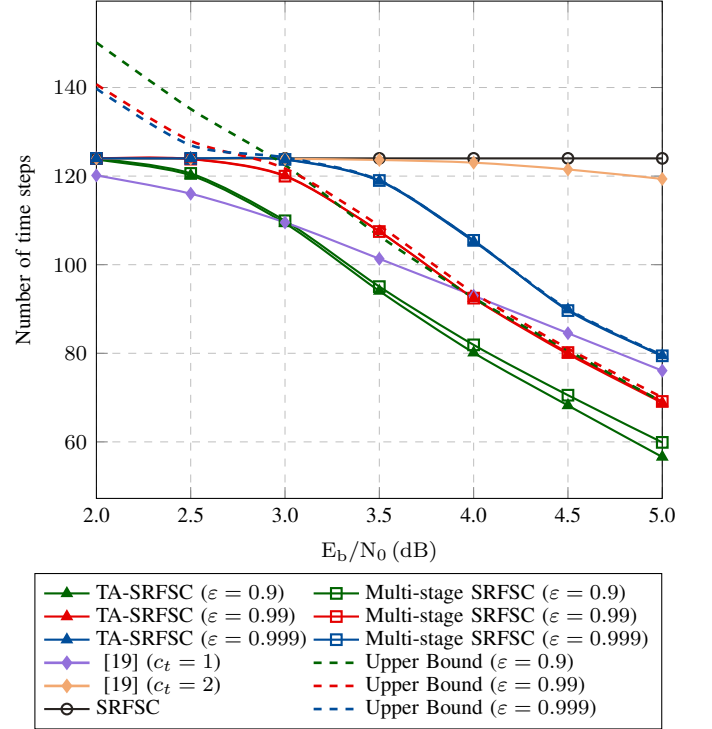


Fig. 10. Average decoding latency of different decoding algorithms for the 5G polar code of length $N = 1024$ and rate $R = 1/2$.

by 21% for $\varepsilon = 0.9$ at $E_b/N_0 = 5$ dB while providing a significantly better BLER/BER performance. Fig. 10 also presents the approximate upper bound derived in (44). It can be seen in the figure that the upper bound in (44) becomes tighter as ε increases.

Fig. 11 compares the average number of threshold comparisons in (29) for the proposed TA-SRFSC decoder with $\varepsilon \in \{0.9, 0.99, 0.999\}$, and the decoder in [19] with $c_t \in \{1, 2\}$. It can be seen that the proposed TA-SRFSC decoder

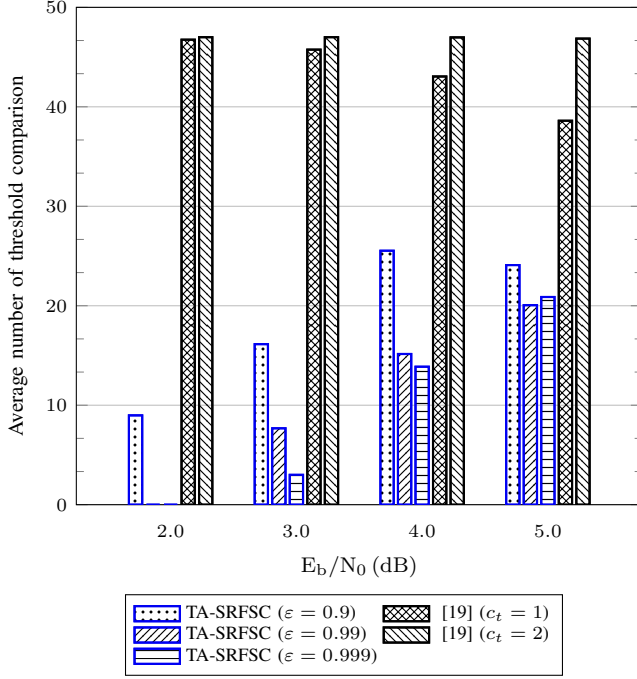


Fig. 11. Average number of threshold comparisons of the proposed TA-SRFSC decoding in comparison with the hard-decision scheme in [19] for the 5G polar code of length $N = 1024$ and rate $R = 1/2$.

shows significant advantage with respect to [19] in terms of the average number of threshold comparisons. The TA-SRFSC decoder with $\epsilon = 0.9$ provides at least 39% reduction with respect to [19] with $c_t = 1$ while having a lower decoding latency. This means the decoder in [19] executes many unnecessary threshold comparison operations, while TA-SRFSC decoding only makes hard decisions when a node satisfies (37).

VII. CONCLUSION

In this work, a new sequence repetition (SR) node is identified in the successive-cancellation (SC) decoding tree of polar codes and an SR node-based fast SC (SRFSC) decoder is proposed. In addition, to speed up the decoding of nodes with no specific structure, the SRFSC decoder is combined with a threshold-based hard-decision-aided (TA) scheme and a multi-stage decoding strategy. We show that this method further reduces the decoding latency without tangibly affecting the error-correction performance when the communications channel has low noise. In particular, simulation results for a polar code of length 1024 and rate 1/2 show that SRFSC decoding obtains up to 19.5% decoding latency reduction with respect to the fastest known decoding algorithm in [17], and the reduction reaches 26.5% at code length 1024 and rate 1/4. In addition, the proposed multi-stage SRFSC decoding reduces the average decoding latency by 54% with respect to SRFSC decoding at $E_b/N_0 = 5$ dB on a polar code of length 1024 and rate 1/2. This average latency saving is particularly important in real-time applications such as video. Future work includes the design of a fast SC list decoder using SR nodes.

APPENDIX A PROOF OF PROPOSITION 1

Let I_k denote the $k \times k$ identity matrix for $k \geq 1$. Since the source node is the rightmost node in an SR node, the g function calculation in (3) can be used as

$$\begin{aligned} \alpha_r^E[1 : 2^r] &= \alpha_j^i[1 : 2^j] \times \left(I_{2^{j-1}} \otimes ((-1)^{\eta_{j-1}}, 1)^T \right) \\ &\quad \times \left(I_{2^{j-2}} \otimes ((-1)^{\eta_{j-2}}, 1)^T \right) \\ &\quad \times \dots \\ &\quad \times \left(I_{2^r} \otimes ((-1)^{\eta_r}, 1)^T \right). \end{aligned}$$

Using the identity $(A \otimes B) \times (C \otimes D) = (A \times C) \otimes (B \times D)$ with $A = I_{2^{j-2}}$, $B = I_2 \otimes ((-1)^{\eta_{j-1}}, 1)^T$, $C = I_{2^{j-2}}$, and $D = ((-1)^{\eta_{j-2}}, 1)^T$ results in

$$\begin{aligned} \alpha_r^E[1 : 2^r] &= \alpha_j^i[1 : 2^j] \\ &\quad \times \left[(I_{2^{j-2}} \times I_{2^{j-2}}) \right. \\ &\quad \left. \otimes \left(I_2 \otimes ((-1)^{\eta_{j-1}}, 1)^T \times ((-1)^{\eta_{j-2}}, 1)^T \right) \right] \\ &\quad \times \left(I_{2^{j-3}} \otimes ((-1)^{\eta_{j-3}}, 1)^T \right) \\ &\quad \times \dots \\ &\quad \times \left(I_{2^r} \otimes ((-1)^{\eta_r}, 1)^T \right), \end{aligned}$$

which can be written as

$$\begin{aligned} \alpha_r^E[1 : 2^r] &= \alpha_j^i[1 : 2^j] \\ &\quad \times I_{2^{j-2}} \otimes \left(((-1)^{\eta_{j-2}}, 1)^T \otimes ((-1)^{\eta_{j-1}}, 1)^T \right) \\ &\quad \times \left(I_{2^{j-3}} \otimes ((-1)^{\eta_{j-3}}, 1)^T \right) \\ &\quad \times \dots \\ &\quad \times \left(I_{2^r} \otimes ((-1)^{\eta_r}, 1)^T \right), \end{aligned}$$

where the identity $I_2 \otimes (a_1, \dots, a_k)^T \times (b_1, b_2)^T = (b_1, b_2)^T \otimes (a_1, \dots, a_k)^T$ is used. Repeating the above procedures results in

$$\begin{aligned} \alpha_r^E[1 : 2^r] &= \alpha_j^i[1 : 2^j] \\ &\quad \times I_{2^r} \otimes \left(((-1)^{\eta_r}, 1)^T \otimes \dots \otimes ((-1)^{\eta_{j-1}}, 1)^T \right) \\ &= \alpha_j^i[1 : 2^j] \\ &\quad \times I_{2^r} \otimes \left((-1)^{s_{i[1]}}, (-1)^{s_{i[2]}}, \dots, (-1)^{s_{i[2^{j-r}]}} \right)^T. \end{aligned}$$

Thus for $k \in \{1, \dots, 2^r\}$,

$$\alpha_{r_l}^E[k] = \sum_{m=1}^{2^{j-r}} \alpha_j^i[(k-1)2^{j-r} + m] (-1)^{s_{i[m]}}.$$

This completes the proof.

APPENDIX B PROOF OF PROPOSITION 2

To prove Proposition 2, a lemma is first introduced as follows.

Lemma 1. For any node \mathcal{N}_j^i whose 2^j bits undergo a hard decision in (29), the probability of correct decoding can be calculated as $(\frac{P_c}{P_e+P_c})^{2^j}$.

Proof: In accordance with Fig. 7, for any node \mathcal{N}_j^i , considering all the previous bits are decoded correctly, the probability that the k -th bit ($1 \leq k \leq 2^j$) in the node undergoes a hard decision is $P_c + P_e$. Moreover, The probability of a correct hard decision for the k -th bit in the node is P_c , regardless of the value of $\beta_j^i[k]$. Thus, the conditional probability that a hard decision on the k -th bit is correct given that the k -th bit undergoes a hard decision is $\frac{P_c}{P_e+P_c}$. Since the LLR values of bits in a node are independent of each other, the conditional probability that hard decisions on all the 2^j bits of node \mathcal{N}_j^i are correct given that all its 2^j bits undergo hard decisions can be calculated as $(\frac{P_c}{P_e+P_c})^{2^j}$. ■

To have a probability of correct decoding of at least ε for all the nodes that undergo hard decision in a polar code of length 2^n , any such node \mathcal{N}_j^i is assumed to have the probability of correct decoding of at least $2^{(n-j)}\sqrt{\varepsilon}$. Under this assumption, even in the worst case that all bits in the code are decoded by hard decision, the correct decoding probability is at least ε . Therefore and by using the result in Lemma 1,

$$\left(\frac{P_c}{P_e+P_c}\right)^{2^j} \geq 2^{(n-j)}\sqrt{\varepsilon}, \quad (45)$$

which is equivalent to

$$\frac{P_c}{P_e+P_c} \geq 2^{n-j}\sqrt{\varepsilon}. \quad (46)$$

If $m_j^i \leq 2c^2$, then $T = -m_j^i + c\sqrt{2m_j^i}$, $P_c = Q(c - \sqrt{2m_j^i})$, and $P_e = Q(c)$. Thus (46) can be written as

$$\frac{1}{2} \left[c - Q^{-1} \left(\frac{Q(c)}{\frac{1}{2^{n-j}\sqrt{\varepsilon}} - 1} \right) \right]^2 \leq m_j^i \leq 2c^2, \quad (47)$$

which requires

$$Q(c) \leq 1 - 2^{n-j}\sqrt{\varepsilon}. \quad (48)$$

If $m_j^i \geq 2c^2$, then $T = m_j^i - c\sqrt{2m_j^i}$, $P_c = Q(-c)$, and $P_e = Q(\sqrt{2m_j^i} - c)$. Thus (46) can be written as

$$m_j^i \geq \max \left\{ 2c^2, \frac{1}{2} \left[c + Q^{-1} \left(\left(\frac{1}{2^{n-j}\sqrt{\varepsilon}} - 1 \right) Q(-c) \right) \right]^2 \right\}. \quad (49)$$

If (48) holds and by using the fact that $Q(-c) = 1 - Q(c)$, then

$$2c^2 \geq \frac{1}{2} \left[c + Q^{-1} \left(\left(\frac{1}{2^{n-j}\sqrt{\varepsilon}} - 1 \right) Q(-c) \right) \right]^2. \quad (50)$$

Thus $m_j^i \geq 2c^2$, which always holds based on the initial assumption. Therefore, it is sufficient to have

$$m_j^i \geq \frac{1}{2} \left[c - Q^{-1} \left(\frac{Q(c)}{\frac{1}{2^{n-j}\sqrt{\varepsilon}} - 1} \right) \right]^2, \quad (51)$$

and (48) to ensure (46). In other words, the probability that all the nodes that undergo hard decision (29) in the decoding

process are decoded correctly will be lower bounded by ε if (48) and (51) are satisfied. Thus, the probability of hard decision error will be upper bounded by $1 - \varepsilon$. This completes the proof.

APPENDIX C PROOF OF PROPOSITION 3

Note that based on Proposition 2, any node \mathcal{N}_j^i that is decoded using (29) has a probability of correct hard decision of at least $2^{(n-j)}\sqrt{\varepsilon}$. For any node that undergoes the SRFSC decoding, the probability of correct decoding is determined by the error rate of SRFSC decoding. Thus, the probability of correct decoding for TA-SRFSC decoding is at least $\varepsilon(1 - \text{BLER}_{\text{SRFSC}})$. Consequently, $\text{BLER}_{\text{TA-SRFSC}} \leq 1 - \varepsilon(1 - \text{BLER}_{\text{SRFSC}})$. This completes the proof.

ACKNOWLEDGMENTS

This work is supported by ERC Proof-of-Concept project BROWSE+; NWO Zwaartekracht program on Integrated Nanophotonics; International collaboration fund of Changchun Institute of Optics, Fine Mechanics and Physics (CIOMP); Open Fund of the State Key Laboratory of Optoelectronic Materials and Technologies (Sun Yat-sen University); and Huawei. In addition, S. A. Hashemi is supported by a Postdoctoral Fellowship from the Natural Sciences and Engineering Research Council of Canada (NSERC).

REFERENCES

- [1] E. Arkan, "Channel polarization: A method for constructing capacity-achieving codes for symmetric binary-input memoryless channels," *IEEE Trans. Inf. Theory*, vol. 55, no. 7, pp. 3051–3073, Jul. 2009.
- [2] 3GPP, "Final report of 3GPP TSG RAN WG1 #87 v1.0.0," Reno, USA, Nov. 2016. [Online]. Available: http://www.3gpp.org/ftp/tsg_ran/WG1_RL1/TSGR1_87.
- [3] K. Niu, K. Chen, J. Lin, and Q. Zhang, "Polar codes: Primary concepts and practical decoding algorithms," *IEEE Commun. Mag.*, vol. 52, no. 7, pp. 192–203, 2014.
- [4] C. Zhang, B. Yuan, and K. K. Parhi, "Reduced-latency SC polar decoder architectures," in *Proc. IEEE Int. Conf. Commun. (ICC)*, Jun. 2012, pp. 3471–3475.
- [5] A. Mishra, A. J. Raymond, L. G. Amaru, G. Sarkis, C. Leroux, P. Meinerzhagen, A. Burg, and W. J. Gross, "A successive cancellation decoder ASIC for a 1024-bit polar code in 180nm cmos," in *Proc. Asian Solid-State Circuits Conf.*, Nov. 2012, pp. 205–208.
- [6] B. Yuan and K. K. Parhi, "Reduced-latency LLR-based SC list decoder for polar codes," in *Proc. 25th Ed. Great Lakes Symp. VLSI*, May. 2015, pp. 107–110.
- [7] —, "Low-latency successive-cancellation list decoders for polar codes with multibit decision," *IEEE Trans. VLSI Syst.*, vol. 23, no. 10, pp. 2268–2280, Oct. 2015.
- [8] G. Sarkis and W. J. Gross, "Increasing the throughput of polar decoders," *IEEE Commun. Lett.*, vol. 17, no. 4, pp. 725–728, Apr. 2013.
- [9] C. Husmann, P. C. Nikolaou, and K. Nikitopoulos, "Reduced latency ml polar decoding via multiple sphere-decoding tree searches," *IEEE Trans. Veh. Technol.*, vol. 67, no. 2, pp. 1835–1839, Feb. 2017.
- [10] A. Alamdar-Yazdi and F. R. Kschischang, "A simplified successive-cancellation decoder for polar codes," *IEEE Commun. Lett.*, vol. 15, no. 12, pp. 1378–1380, Dec. 2011.
- [11] G. Sarkis, P. Giard, A. Vardy, C. Thibault, and W. J. Gross, "Fast polar decoders: Algorithm and implementation," *IEEE J. Sel. Areas Commun.*, vol. 32, no. 5, pp. 946–957, May. 2014.
- [12] Z. Huang, C. Diao, and M. Chen, "Latency reduced method for modified successive cancellation decoding of polar codes," *Electron. Lett.*, vol. 48, no. 23, pp. 1505–1506, Nov. 2012.

- [13] A. Balatsoukas-Stimming, G. Karakostas, and A. Burg, "Enabling complexity-performance trade-offs for successive cancellation decoding of polar codes," in *Proc. IEEE Int. Symp. Inf. Theory Process. (ISIT)*, Jun. 2014, pp. 2977–2981.
- [14] L. Zhang, Z. Zhang, X. Wang, C. Zhong, and L. Ping, "Simplified successive-cancellation decoding using information set reselection for polar codes with arbitrary blocklength," *IET Commun.*, vol. 9, no. 11, pp. 1380–1387, Jul. 2015.
- [15] P. Giard, A. Balatsoukas-Stimming, G. Sarkis, C. Thibault, and W. J. Gross, "Fast low-complexity decoders for low-rate polar codes," *J. Sign. Process. Syst.*, vol. 90, no. 5, pp. 675–685, May. 2018.
- [16] M. Hanif and M. Ardakani, "Fast successive-cancellation decoding of polar codes: identification and decoding of new nodes," *IEEE Commun. Lett.*, vol. 21, no. 11, pp. 2360–2363, Nov. 2017.
- [17] C. Condo, V. Bioglio, and I. Land, "Generalized fast decoding of polar codes," in *Proc. IEEE Global Commun. Conf. (GLOBECOM)*, Dec. 2018, pp. 1–6.
- [18] H. Gamage, V. Ranasinghe, N. Rajatheva, and M. Latva-aho, "Low latency decoder for short blocklength polar codes," *arXiv preprint arXiv:1911.03201*, 2019.
- [19] S. Li, Y. Deng, L. Lu, J. Liu, and T. Huang, "A low-latency simplified successive cancellation decoder for polar codes based on node error probability," *IEEE Commun. Lett.*, vol. 22, no. 12, pp. 2439–2442, Dec. 2018.
- [20] H. Sun, R. Liu, and C. Gao, "A simplified decoding method of polar codes based on hypothesis testing," *IEEE Commun. Lett.*, pp. 1–1, Jan. 2020.
- [21] C. Leroux, I. Tal, A. Vardy, and W. J. Gross, "Hardware architectures for successive cancellation decoding of polar codes," in *Proc. IEEE Int. Conf. Acoust., Speech Signal Process.*, May. 2011, pp. 1665–1668.
- [22] R. Silverman and M. Balser, "Coding for constant-data-rate systems," *Trans. IRE Prof. Group Inf. Theory*, vol. 4, no. 4, pp. 50–63, Sep. 1954.
- [23] P. Trifonov, "Efficient design and decoding of polar codes," *IEEE Trans. Commun.*, vol. 60, no. 11, pp. 3221–3227, Nov. 2012.
- [24] Z. Zhang and L. Zhang, "A split-reduced successive cancellation list decoder for polar codes," *IEEE J. Sel. Areas Commun.*, vol. 34, no. 2, pp. 292–302, Feb. 2016.
- [25] M. El-Khamy, J. Lee, and I. Kang, "Detection analysis of CRC-assisted decoding," *IEEE Commun. Lett.*, vol. 19, no. 3, pp. 483–486, Mar. 2015.
- [26] 3GPP, "3GPP TS RAN 38.212 v1.2.1," Dec. 2017. [Online]. Available: http://www.3gpp.org/ftp/Specs/archive/38_series/38.212/38212-f30.zip.